Evaluation of Dynamic Vapour Sorption Isotherms Characteristics of Small Cardamom (Elettaria cardamomum Maton) using Empirical and Neural Network Models

Sushreesmita Mishra
Indian Institute of Technology Delhi
Jatindra K Sahu (jksahu@iitd.ac.in)
Indian Institute of Technology Delhi
Nitya Sharma
Indian Institute of Technology Delhi
Ankur Kumar
National Institute of Food Technology Entrepreneurship and Management

Research Article

Keywords: Small cardamom, Dynamic vapour sorption, Artificial neural network, Isosteric heat of sorption, Glass transition temperature

Posted Date: May 15th, 2023

DOI: https://doi.org/10.21203/rs.3.rs-2902609/v1

Abstract

Moisture sorption isotherm (MSI) characteristics of small cardamom *(Elettaria cardamomum* Maton) capsules were determined over water activity (a_w) ranging from 10 to 90% at 20, 30, and 40°C using dynamic vapour sorption method. Equilibrium moisture contents (EMC) were correlated by three empirical models and multilayer neural network approach. It was observed that the Caurie model fitted best among empirical models for predicting EMC values. However, artificial neural network (ANN) model having 15 hidden neurons optimized using Lavenberg-Marquardth training algorithm was superior to the empirical models with the highest coefficient of determination (R^2) value of 0.995 and 0.993 for adsorption and desorption respectively. Monolayer moisture content (M_m) determined by the Caurie model was found to be 2.167, 1.901, AND 1.828% dry basis (*db)* for adsorption, and 3.133, 3.061, and 2.744% (*db*) for desorption at 20, 30 and 40°C, respectively. Net isosteric heat of sorption (q_{st}), sorption entropy and Gibb's free energy (ΔG) change were found to be inversely related to the EMC values. Glass transition temperature (T_g) was found to be 98.91°C. The critical moisture content (CMC) and critical water activity of cardamom from T_g-a_w-EMC relationship was observed to be 1.989% (*db*) and 0.766, respectively at 30°C.

1. Introduction

Cardamom *(Elettaria cardamomum* Maton) is widely used for the domestic culinary purposes due to its pleasant aroma and subtle pungent flavour. Essential oil of small cardamom finds its extensive utilization in pharmaceutical and nutraceutical industries owing to the presence of various natural immune-boosting functional phytochemicals (Amma et al. 2010). Small cardamoms are susceptible to microbial spoilage, if a_w value of air surrounding the storage environment exceeds the safe storage limit. Stringent control of temperature and a_w should be maintained to ensure the longer shelf life of cardamom capsules.

Drying of cardamom capsules to CMC helps in prevention of oxidation of essential oils and spoilage caused due to enzymatic and microbial activity, thereby preserves aroma and colour of cardamoms. Proper drying technology and storage conditions can be established by determining such critical values, which can be determined by analysis of MSIs at different temperature and a_w values. Further, MSI study provides an insight about prediction of shelf-life, estimation of moisture variation during storage and subsequent handling and packaging, drying kinetics, and optimizing process design and development of appropriate drying equipment (Yogendrarajah et al. 2015). In MSI study, CMC used for evaluating above thermodynamic properties are generally calculated from two and three parameter empirical models such as Guggenheim-Anderson-de Boer (GAB), Brunauer-Emmett-Teller (BET) and Caurie models. These models evaluates M_m which is considered as a critical parameter for estimating optimum moisture content for extended storage life (Marcos et al. 1997). The moisture content below M_m is bound to the product and does not contribute for any microbial activities leading to deterioration of food (Andrade et al. 2011).

Application of ANN provides better solution for optimizing sorption kinetics than conventional empirical equations which solves moisture sorption isotherm problem by non-linear regression approach. Additionally, ANN can address both linear as well as nonlinear relationship between measured input and network outputs. Nevertheless, ANN doesn't give information about physical parameters like other empirical models; it has ability to learn from experimental values handling complex system in a single model (Corrêa et al. 2010). ANN has been successfully applied for optimization of various post-harvest processes as well for predicting equilibrium moisture content in sorption isotherm studies (Al-Mahasneh et al. 2014; Mahanti et al. 2019; Panchariya et al. 2002).

Although moisture sorption behavior provides information relating to storage stability of food products, it does not provide in depth understanding about many physical changes such as crystallization, stickiness, crispiness, and rate of nonenzymatic browning. Thermodynamic properties of foods such as enthalpy, entropy, free energy, and glass transition temperature set forth essential information about sorption mechanism as well as food-water interactions in a food. Below glass transition temperature, a food product is considered to be shelf stable for storage. So far, no study has been reported on MSI of small cardamom to define its appropriate storage and packaging conditions and systems. Therefore, this study was undertaken to (i) evaluate the sorption (adsorption and desorption) isotherms of small cardamom at 20, 30 and 40°C, (ii) describe the experimental data by assessing the empirical and neural network models, and (iii) evaluate thermodynamic properties of sorbed water.

2. Material and Methods

2.1 Raw material

Small cardamom capsules used in this study were of *Njallani* variety procured from Wayanad district (11.6854° N, 76.1320° E) of Kerala, India. The samples were soaked in sodium carbonate solution (0.1% w/v for 15 min) immediately after harvest to remove the extraneous foreign materials. The average moisture content of the samples was 7.8 ± 1.2% wet basis (*wb*). The samples were dried in a hot-air drier (Jaisbo, Delhi) at 50°C for 32 h to shorten the equilibrium time prior to experiment.

2.2 Measurement of MSIs

The MSIs of cardamom samples were determined using a Moisture Sorption Analyzer (DVS-1000 Gravimetric, Surface Measurement Systems Ltd., London). The instrument comprised of a temperature and humidity-controlled chamber holding a microbalance with two sample crucibles (reference and sample) and a system for humidification (Fig. 1). The atmosphere was regulated by circulating dry and wet stream of nitrogen gas through the crucibles, which was monitored using two electronic mass flow controllers. The sorption process in the apparatus was controlled by a computer, where stepwise variation in a_w at a set temperature was pre-programmed.

Sorption isotherms of the capsules were obtained at 20, 30 and 40°C at a_w values ranging from 10 to 90% at 10% stepwise increment and a_w then decreased in a similar manner. A fixed $\left(\frac{dm}{dt}\right)$(mass variation over time) of 0.0002% min^{-1} was selected for all experiments. A maximum stage time of 360 min and a minimum of 10 min were selected for all experiments. The mass in equilibrium at specific temperature and a_w was obtained by identifying the corresponding mass at the end of each a_w step, which was further used for evaluating the sample moisture content, based on its dry mass. Adsorption and desorption isotherm plots were produced using this calculated EMC values at the temperature and a_w. In this experiment about 123.138, 125.565, and 176.258 mg of pre-dried cardamom samples were used at 20, 30 and 40°C, respectively.

2.3 Model fitting of sorption isotherms

The BET, GAB and Caurie moisture sorption models were fitted to experimental moisture sorption data at 20, 30 and 40°C (Table 1). ANN was used to predict EMCs as it provides better modelling result compared to empirical models and has successfully been used for predicting water sorption isotherms of brown rice (Mahanti et al. 2019), safflower seed (Barati et al. 2016), legumes and cereal grains (Al-Mahasneh et al. 2014) and maize (Chayjan and Esna-Ashari 2010). The Multi-Layer Perception (MLP) network used in the present study had two input variables (a_w and temperature), one hidden layer having fifteen neurons and one output layer representing EMC (Fig. 2). The number of hidden layer neurons was decided by hit and trial and error based on the highest correlation between measured output and network output variables, since large number of neurons in the hidden layer may require more training time and over-fitting, whereas limited neurons in hidden layer may lead to under-fitting. In total, 27 combinations from this input variables were collected for modeling; out of which 60% data were used for network training, 20% for network validation and 20% for network testing, randomly selected from whole data set. Lavenberg–Marquardt (LM) algorithm was used to train ANN. Threshold function TANSIG was used for training the experimental data using feed forward back propagation neural networks (Eq. 1). The mean sum of squares (MSE) of network errors was used to determine the performance function during training of feed-forward neural networks. Neural network toolbox of MATLAB (Matlab 2018b) was used in this study.

Table 1
Models fitted to sorption isotherm data of small cardamom

Model	Equation	References
BET	$\frac{M_c}{M_m}=\frac{C_b a_w}{(1-a_w)(1-a_w+C_b a_w)}$	(Chirife & Iglesias, 1978; Iglesias & Chirife, 1976)
GAB	$\frac{M_c}{M_m}=\frac{C_g K a_w}{(1-Ka_w)(1-Ka_w+KC_g a_w)}$	(van den Berg & Bruin, 1981)
Caurie	$\frac{1}{M_c}=\frac{1}{C_c M_m}\left(\frac{1-a_w}{a_w}\right)^{\left(\frac{2C_c}{M_m}\right)}$	(Caurie, 1981)
M_c: equilibrium moisture content (% *db*); M_m, monolayer moisture content (% *db*); $C_b, C_g, \text{and} C_c$: BET, GAB and Caurie constants respectively; T: Temperature (°C); and a_w: water activity		

$$Y_j = 2/(1+\exp\left(-2X_j\right)) - 1$$

1

where, Y_j is weighted output and X_j is sum of weighted inputs for each neuron ion *j*th layer.

2.4 Properties of sorbed moisture

The Caurie model represents the calculation of number of adsorbed monolayer (*N*), sorbed water density (*ρ*) and adsorbent surface area (*A*) (Dalgıç et al. 2012). The value of *N* for cardamom capsule was determined using the following equation.

$$N = \frac{M_m}{C_c}$$

2

where M_m is the monolayer moisture content obtained from the Caurie's model and C_c is the Caurie's constant. Within the monolayer M_m, *ρ* is considered equal to the magnitude of C_c and therefore, the surface area of adsorbent (*A*) was evaluated as follows.

$$A = \frac{M_m}{C_c \times d \times 10^8}$$

3

where *d* is the diameter of water molecule (3.673 x 10^{-10} m).

2.5 Isosteric heat of sorption and sorption entropy

Thermal properties of sorbed water describe relationship between food matrix and its moisture content. Clausius-Clapeyron equation (Eq. 4) was used to calculate the net and total isosteric heat of sorption to estimate intermolecular force of attraction between sorption sites and moisture content (Yogendrarajah et al. 2015).

$$\left[\frac{d\ln\left(a_w\right)}{d\left(T\right)}\right]_{Mc} = \frac{q_{st}}{RT^2}$$

4

where, a_w is relative humidity (%), T is absolute temperature (K), q_{st} is net isosteric heat of sorption (kJ.kg^{-1}) and R is universal gas constant (8.314 kJ mol$^{-1}K^{-1}$). The value of M_c is assumed up to monolayer value M_m according to the value derived from the best-fitted sorption model. Assuming q_{st} is independent of temperature and integrating Eq. (4),

$$-\ln(a_w) = \left({}^{q_{st}}/_{RT}\right) + C \qquad (5)$$

where C is intercept of the straight line obtained using Eq. (7). The slope of the linear graph between ln(a_w) and 1/T was used to calculate the value of q_{st}, where a_w is the corresponding value of M_c from the best-fitted model.

The total heat of sorption (Q_{st}), which is physically associated to amount of energy required in a drying process, was estimated from the following relationship (Toǧrul and Arslan 2007).

$$Q_{st} = q_{st} + \triangle H_{vap}$$

6

where, ΔH_{vap} is heat of vapourisation of pure water at 30°C, which is the mean temperature used in this study.

The sorption entropy change (ΔS) was determined from equating intercept obtained from the straight line obtained from Eq. (5) to $\Delta S/R$ (Barati et al. 2016). Sorption entropy or degree of randomness of any specific product helps to infer different chemical process such as dissolution and crystallization. This corresponds to the attraction-repulsive forces inside a system, as it depends on the number of available sorption sites at a specific energy level (Toǧrul and Arslan 2007).

2.6 Enthalpy-entropy compensation theory

Several studies have investigated the role of enthalpy-entropy compensation theory in many physical and chemical processes (McMinn et al. 2005), which projects a linear relationship between Q_{st} and ΔS.

$$Q_{st} = T_\beta \triangle S + \alpha$$

7

The linear regression straight line obtained between Q_{st} and ΔS, was used to calculate isokinetic temperature (T_β) and constant (α). The isokinetic temperature indicates the temperature at which all reactions have the same reactivity in a specific condition. A compensation pattern only exists when there is enthalpy and entropy follow a linear correlation and T_β is not equal to the harmonic mean temperature (T_{hm}).

$$T_{hm} = \frac{n_s}{\sum_{i=1}^{n_s}\left(\frac{1}{T}\right)}$$

8

where n_s is the number of isotherms or temperature level. If $T_\beta > T_{hm}$ the process is enthalpy driven, while the reverse ($T_\beta > T_{hm}$) is considered to be entropy controlled.

2.7 Gibb's free energy change

Gibb's free energy change (ΔG) indicates the sorbent's affinity towards water, that specifies the nature of the water sorption process is spontaneous or not depending on the sign of ΔG value (McMinn et al. 2005). Negative values (- ΔG) implies that the water sorption process is spontaneous, while positive value (+ΔG) implies non-spontaneity. Free energy changes in small cardamom caused by change in moisture was calculated by Eq. (9).

$$\triangle G = -RT\ln\left(a_w\right)$$

9

Free energy change at several EMCs for each temperature was calculated using the values of a_w generated by the Caurie model.

2.8 Glass transition temperature

The glass transition temperature of the samples conditioned at different moisture content was evaluated by using a differential scanning calorimetry (DSC 200 F3, Netzsch) equipped with a built-in software (DSC 200 F3 1-414/6 for measurement and Proteus for post-analysis). The instrument was calibrated using Indium. Approximately, 1 g of cardamom powder equilibrated at a range of water activities (0.1 to 0.9) were weighted in an aluminum sample pan and hermetically sealed. A similar empty pan was used as reference. The samples were scanned from room temperature to 150°C at a speed of 10 K heating rate, 30 points/K acquisition rate. Nitrogen was used as a purge gas with protective MFC at the flow rate of 20ml/min. Each DSC thermographs were acquired to analyze onset (T_o), middle (T_g) and conclusion temperature (T_c) out of which T_g was considered as glass transition temperature. All measurements were made in duplicate. Further, the experimental T_g-a_w curve was fitted using known Khalloufi, Maslouhi and Ratti (KMR) model (Khalloufi et al. 2000).

$$T_g = \frac{A{a_w}^2 + Ba_w + T_{gs}}{a{a_w}^2 + ba_w + 1}$$

10

where, T_{gs} is glass transition temperature of anhydrous solid, and *A, B, a, b* are parameters of KMR model.

2.8 Statistical analysis

The goodness of fit and model parameters were evaluated using non-linear least square method in MATLAB (2018b, Mathworks, Inc.). The highest value of R^2 and lowest value of root mean square error (*RMSE*) were used to judge the model fitting. One-way ANOVA was applied to the experimental data for multiple comparisons. Level of significance (*p*) was calculated at 5%.

$$R^2 = 1 - \frac{\sum_{i=1}^{n}\left(M_c - M_{c,p}\right)}{\sum_{i=1}^{n}\left(M_c - \sum_i \frac{M_c}{n}\right)}$$

11

$$RMSE = \left[\frac{1}{n}\sum_{i=1}^{n}\left(M_c - M_{c,p}\right)\right]^{0.5}$$

12

where, M_c and $M_{c,p}$ are experimental and predicated values of EMC, respectively, and *n* is number of observations.

3. Results and Discussion

3.1 Temporal moisture sorption profile

Figure 3 showed the temporal profile of mass of cardamom samples for both adsorption and desorption processes using a DVS analyser at 20, 30 and 40°C. It is apparent that mass of cardamom samples increased during adsorption when a_w increased stepwise, and then decreased during stepwise reduction of a_w. Almost all the selected a_w and equilibrium was reached within about 6 h for all the experimental runs. The experimental values of EMC obtained at each a_w step for small cardamom is depicted in Fig. 4. Earlier studies indicated that the experimental times necessary to reach the equilibration conditions are significantly lower (40–60%) than the time taken in the conventional gravimetric method i.e. saturated salt solution (SSS) method (2 ± 3 weeks) (Penner and Schmidt, 2013). In another study, there was visible mold growth for corn starch, soy protein, microcrystalline cellulose, sucrose and corn flakes at higher a_w values during determination of moisture sorption isotherm by SSS method (Schmidt and Lee 2011). Further, the SSS method requires manual data collection which often associated with experimental error. Therefore, DVS analyser overcomes the disadvantage of SSS method.

3.2 Moisture sorption isotherms

The profile of MSI gives insight about hygroscopicity of the product; steep isotherm is obtained for highly hygroscopic product while a flat isotherm is obtained for weakly hygroscopic product. As observed in Fig. 4, the MSIs obtained exhibited BET III type isotherm characteristics. The figure shows that the percentage increase in EMC was lower at moderate and intermediate a_w values and increased distinctly at higher a_w values. At lower relative humidity, moisture was absorbed only at the external surface sites, which enables only small amount of water sorption. With increase in relative humidity, dissolution of soluble components causes increase in moisture content. These type of isotherms are common for most agricultural products having rich water soluble components mainly carbohydrates (Lomauro et al. 1985). BET III type or “J shape” isotherm exists when binding between water molecules exceeds the binding energy of first layer (Al-Muhtaseb et al. 2002). Similar trends are also reported for other spices, for instance, mint (Dalgıç et al. 2012) and black pepper (Yogendrarajah et al. 2015).

It was observed that there was a significant ($p < 0.05$) difference between desorption and adsorption isotherm curves (Fig. 4) which indicates a clear hysteresis. This hysteresis might be due to the change in hygroscopicity of cardamom samples during adsorption and desorption process. The hysteresis is a measure of available sorption sites in a product (Sahu et al. 2018). Additionally, the sorption hysteresis of cardamom could be due to the unique mechanism of binding-together of sorption sites during desorption to satisfy each other rather than forming hydrogen bonds to water molecules. The hygroscopicity is lowered consequently during adsorption due to the saturation attained by number of sorption sites by each other in a favourable way which leads to reduction of amount of available sorption sites resulting in a lower hygroscopicity and lower moisture content at a given humidity.

3.3 Temperature dependence of isotherms

Figure 5 reveals that the temperature influences the adsorption and desorption isotherms for the entire range of a_w. At a specific a_w, a decrease in most of EMC values was observed with increase in temperature, which might be possibly due to the presence of more water binding natural molecules, for instance, carbohydrate and proteins. Therefore, small cardamom became less hygroscopic at higher temperatures. Effect of temperatures was found to be significant ($p < 0.05$) on EMC at all temperature range. Furthermore, the MSIs were found to overlap at specific a_w. The overlapping of sorption curves at different temperature have also been reported for black pepper, grapes and apricot (Kaymak-Ertekin and Gedik, 2004; Yogendrarajah et al. 2015).

3.4 Fitting of empirical and neural network models to experimental data

The values of R^2, *RMSE*, and model constants were presented in Table 2. The value of R^2 was used as an indicator of the fitness of the models. The Caurie model explained the most accurate fit to the most of the experimental sorption data, with R^2 values 0.992, 0.982 and 0.985 during adsorption, and 0.988, 0.986 and 0.978 during desorption at 20, 30 and 40°C, respectively. However, the GAB and BET model showed a poor fit to the data with a maximum R^2 value of 0.794. Soysal and Oztekin (1999) compiled data set for EMC-a_w relationship for 13 different spices and herbs including cardamom, where they concluded that the Oswin model produced the best fit than the Henderson and Halsey models. The values of M_m calculated using the best-fitted Caurie model were: 2.167, 1.901, and 1.828% (*db)* for adsorption, and 3.133, 3.061, and 2.744% (*db*) for desorption at 20, 30 and 40°C, respectively. M_m is an important parameter which decides the shelf life of products. Below M_m value, most of the biodegradation process, spoilage reaction and physical changes such as loss of crispiness and caking occurs. Also the value of M_m indicates the amount of water that is absorbed by a single layer to the binding sites of the food product (Arslan-Tontul 2021). A decrease in M_m values with an increase in temperature was observed for small cardamom samples. The reason behind this phenomenon is that at elevated temperature the binding energy in water molecules decreases as a result of differentiating attractive forces between sorption sites and water molecules, leading to increase in molecules distances. Subsequently, temperature induced chemical and physical changes cause a significant reduction in number of active sites or hydrogen bonds. Furthermore, the estimated values of the Caurie constant C_c for adsorption was lower than for the desorption. These findings are consistent with results published on red pepper, onion and cinnamon (Rhim and Hong, 2011; Alam and Islam, 2015; Bernardino-Nicanor and González-Cruz, 2016).

Table 2
Estimated coefficients and accuracy of fit of sorption isotherm models

Sorption Model		Adsorption			Desorption		
	Constants	20°C	30°C	40°C	20°C	30°C	40°C
Caurie	M_m	2.167	1.901	1.828	3.133	3.061	2.744
	C_c	0.969	1.037	0.924	1.159	1.155	1.039
	R^2	**0.992**	**0.985**	**0.982**	**0.988**	**0.986**	**0.978**
	RMSE	0.580	0.785	0.673	0.682	0.739	0.757
GAB	M_m	0.010	0.005	0.007	0.021	3.556	0.002
	C_g	0.480	0.482	0.481	0.497	0.499	0.502
	K	2.351	2.359	2.360	2.444	2.458	2.463
	R^2	0.049	0.030	0.054	0.100	0.792	0.108
	RMSE	7.238	6.910	5.802	7.955	1.463	6.325
BET	M_m	-0.001	-0.001	-0.001	-0.002	0.192	0.000
	C_b	-4.411	-4.394	-4.411	-4.854	50.722	-4.871
	R^2	0.056	0.060	0.061	0.026	0.794	0.001
	RMSE	0.244	0.204	0.226	1.189	0.889	0.730
ANN model	*RMSE*	**0.997**	**0.999**	**0.995**	**0.996**	**0.995**	**0.986**

In the present study, the suitability of ANN model was analyzed by comparing the predicted and experimental values of EMC obtained for small cardamom. Table 2 indicated that the value of R^2 for predicting EMC values were 0.997, 0.999 and 0.995 for adsorption, and 0.996, 0.995, and 0.986 for desorption at 20, 30 and 40°C, respectively. Thus, within the temperature range ANN model predicted the EMC values better than the empirical models. Although EMCs are not commonly evaluated using ANN models, however, the ability of this model to accurately analyze a wide range of data, make it a potential method. Al-Mahasneh et al. (2014) collected data of MSI of twelve cereals and five legumes from literature and developed an ANN model to predict EMC taking input variables as product type (grains or legumes), sorption state (adsorption or desorption), temperature and EMC. In this study, comparable overall prediction results were obtained using both ANN and conventional analytical MSI model (Fig. 6). In a study conducted by Correa et al. (2010), ANN model was found to predict EMCs of coffee beans accurately during desorption with a temperature range of 10 to 50°C and a_w ranging from 11 to 95%.

3.5 Thermodynamic properties

3.5.1 Properties of sorbed water

The number of adsorbed monolayers for cardamom samples evaluated using M_m values from the Caurie model were 1.89, 2.06, and 2.09, and 2.70, 2.65, and 2.64 for adsorption and desorption at 20, 30 and 40°C respectively. The adsorbed monolayers of cardamom were found to increase with increasing temperature, that may be due to the presence of polar groups (Dalgıç et al. 2012). The adsorption surface areas of small cardamom were calculated to be 51.34, 56.03 and 56.89 m^2 g^{-1} solid at 20, 30 and 40°C respectively, and the desorption surface area were 73.59, 72.13 and 71.92 m^2 g^{-1} solid at 20, 30 and 40°C respectively. The properties of bound water and surface area of adsorbent was significantly influenced by the change in temperature (Sawhney et al. 2014). Sorption specific area of cardamom samples appeared to be reduced with increase in temperature during adsorption and desorption. Further, both adsorbed monolayer and surface area of adsorbent was lower than desorption during adsorption.

3.5.2 Isosteric heat of sorption and sorption entropy

Isosteric heat Q_{st} was highly dependent on EMC values and decreased exponentially with moisture content (Fig. 7). This could be because of available sites for moisture sorption become occupied with sorption time, resulting in the reduction of Q_{st} values. At lower moisture content there is a greater number of active polar sites on the surface of the product, leading to higher Q_{st} value at low moisture content. For adsorption and desorption, the maximum Q_{st} was found to be 101.67 J mol^{-1} and 156.19 J mol^{-1}, respectively. As expected, at lower EMCs, the values of total isosteric heat Q_{st} of desorption was higher than that of adsorption which indicates that the heat energy released during desorption was higher than the energy released during adsorption. However, at higher EMC values, this difference was found to be decreasing. Moreover, the magnitude of heat of sorption at a specific moisture content could predict the state of adsorbed water, that would help in detecting and understanding physical, chemical, and microbiological stability of small cardamom. Eqs. 12 and 13 show the dependency of Q_{st} on EMC values of small cardamom.

Adsorption: $Q_{st} = 11.28\exp(-0.26EMC)$ (R^2 = 0.974) (12)

Desorption: $Q_{st} = 6.79\exp(-0.21EMC)$ (R^2 = 0.974) (13)

The sorption entropy (ΔS) follows similar trend to q_{st} i.e., systems entropy showed an inverse dependence with moisture content. The maximum value of ΔS was calculated as 6.18 J mol^{-1} and 10.09 J mol^{-1} during adsorption and desorption respectively.

3.5.3 Enthalpy-entropy compensation theory

The isokinetic theory or enthalpy-entropy compensation theory assists in evaluation of sorption reactions, whether the reaction is driven by enthalpy or entropy. This could be established by comparing harmonic temperature (T_{hm}) and isokinetic temperature (T_{β}) to predict the existence of true compensation. The relation between ΔS and Q_{st} (Fig. 8) for cardamom sample was found to be linear with R^2 values of 0.947 and 0.945 for adsorption and desorption respectively. Hence, it could be concluded that enthalpy and entropy comprehended true compensation amongst each other. Further, the value of T_{hm} was found out to be 302.779 K which is lower than the isokinetic temperatures during adsorption (323.81 K) and desorption (344.85 K). Therefore, it was concluded that the moisture sorption process in this study was enthalpy driven.

3.5.4 Gibb's free energy change

Figure 9 shows the varying change in Gibbs free energy (-ΔG) with EMC values. The values of ΔG decreased exponentially with EMC which explained spontaneity of water adsorption and desorption processes. The Gibbs free energy change ranged from 152.767 to 558.603 J mol^{-1} and 210.503 to 920.080 J mol^{-1} for adsorption and desorption respectively. According to Sharma et al. (2018), higher values of -ΔG during desorption indicated hydrophilic nature of a food material, small cardamom in the present study.

3.6 Glass transition and product stability

Glass transition temperature (T_g) of cardamom samples at different water activity values were obtained using DSC thermographs to evaluate moisture-based storage stability of the product. The values of T_g decreased from 95°C to 42°C with increase in water activities from 0.1 to 0.9. The data fitted to the KMR equation (Eq. 10) demonstrated a better fit with an R^2 value of 0.991 and corresponding parameters are shown in Table 3. The value of T_{gs} obtained from KMR model was found out to be 98.91°C. The combination of glass transition theory and water activity along with EMC values is portrayed in Fig. 10. This state diagram can help in determining CMC and critical water activity of cardamom capsules and furthermore can be proposed as limiting value at which physical transformations like stickiness, caking, and crystallization occur. The values of EMC with respect to a_w were obtained at its storage temperature (30°C) from best fitted model i.e., the Caurie model in the present study. The CMC and critical a_w was found to be 1.989% (*db*) and 0.766. This suggests that at 30°C, cardamom capsules can be stored in glassy state at water activity less than 0.76 and moisture content of 1.98% (*db*). Interestingly, the value of M_m (1.901%, *db*) obtained from the Caurie model is less than this CMC value implying that the quality of cardamom sample was not dominated by the plasticizing effect of water.

Table 3
Nonlinear regression parameters of KMR model for small cardamom

Parameters		Goodness of fit	
A	120	SSE	24.56
B	-221	R^2	0.991
Tgs	98.91	Adjusted R^2	0.982
a	0.900	RMSE	2.478
b	-1.994		

5. Conclusion

The sorption behaviour of small cardamom were investigated using dynamic vapour sorption isotherm. The sorption isotherm showed type III curve according BET classification. The EMC curve for adsorption was lower than desorption showing a hysteresis effect. Among empirical models, the Caurie model was found to be satisfactory for the prediction of moisture adsorption isotherm over entire values of relative humidity. ANN model was used to predict EMCs of small cardamom with superior model fitting. There was increase in adsorbed monolayers and sorption surface area with increasing temperature. With increasing moisture content of small cardamom, there was a reduction in heat of sorption and sorption entropy, leading to a decrease in binding energy for removal of water. A true enthalpy-entropy compensation theory existed, and moisture sorption reaction was found to be enthalpy driven. Higher Gibb's free energy change during desorption indicated a higher tendency of water uptake by small cardamom. Additionally, the combined analysis of T_g-a_w-EMC, provided a better knowledge regarding physical and thermodynamics properties of small cardamom.

Declarations

Authors contribution: Sushreesmita Mishra: Conceptualization, Experimentation, Data Curation, Data Analysis, Writing-Original draft. **Jatindra K Sahu:** Supervision, Editing, Reviewing, Resource arrangement. **Nitya Sharma**: Reviewing, formal analysis. **Ankur Kumar**: Experimentation.

Acknowledgement: Authors would like to thank Science and Engineering Research Board, Govt. of India for funding the study. Sincere thanks to IIT Bombay for providing DVS analyzer facilities.

Ethical approval: Not applicable

Consent for publication: All authors gave their consent for publication of the manuscript.

Funding: This work was supported by Science and Engineering Research Board, Govt. of India (Sanction no. YSS/2015/001756).

Availability of data and materials: Data will be available on request.

Conflict of interest: The authors declare that they have no known competing financial or non-financial interests.

References

1. Al-Mahasneh, M., Alkoaik, F., Khalil, A., Al-Mahasneh, A., El-Waziry, A., Fulleros, R., Rababah, T.: A generic method for determining moisture sorption isotherms of cereal grains and legumes using artificial neural networks. J. Food Process Eng. 37, 308–316 (2014). https://doi.org/10.1111/jfpe.12087
2. Al-Muhtaseb, A.H., McMinn, W.A.M., Magee, T.R.A.: Moisture Sorption Isotherm Characteristics of Food Products: A Review. Food Bioprod. Process. 80, 118–128 (2002). https://doi.org/10.1205/09603080252938753
3. Alam, M.M., Islam, M.N.: Study on water sorption isotherm of summer onion. Bangladesh J. Agric. Res. 40, 35–51 (2015). https://doi.org/10.3329/bjar.v40i1.23753
4. Amma, K.P.A.P., Rani, M.P., Sasidharan, I., Nisha, V.N.P.: Chemical composition, flavonoid - phenolic contents and radical scavenging activity of four major varieties of cardamom. Int J Biol Med Res. 1, 20–24 (2010)
5. Andrade, R.D., Lemus, R., Perez, C.E.: Models of Sorption Isotherms for Food: Uses and Limitations. Vitae-Revista La Fac. Quim. Farm. 18, 324–333 (2011)
6. Arslan-Tontul, S.: Moisture sorption isotherm and thermodynamic analysis of quinoa grains. Heat Mass Transf. 57, 543–550 (2021). https://doi.org/10.1007/s00231-020-02978-8
7. Barati, M., Zare, D., Zomorodian, A.: Moisture sorption isotherms and thermodynamic properties of safflower seed using empirical and neural network models. J. Food Meas. Charact. 10, 236–246 (2016). https://doi.org/10.1007/s11694-015-9298-4
8. Bernardino-Nicanor, A., González-Cruz, L.: Thermodynamic Analysis of Cinnamon Sorption Isotherms (Cinnamomum zeylanicum). Adv. Biores. 7, 75–83 (2016). https://doi.org/10.15515/abr.0976-4585.7.1.7583
9. Chayjan, R.A., Esna-Ashari, M.: Modeling of heat and entropy sorption of maize (cv. Sc704): Neural network method. Res. Agric. Eng. 56, 69–76 (2010). https://doi.org/10.17221/37/2009-rae
10. Dalgıç, A.C., Pekmez, H., Kadir, &, Belibağlı, B.: Effect of drying methods on the moisture sorption isotherms and thermodynamic properties of mint leaves. J. Food Sci. Technol. 49, 439–449 (2012). https://doi.org/10.1007/s13197-011-0302-7
11. Kaymak-Ertekin, F., Gedik, A.: Sorption isotherms and isosteric heat of sorption for grapes, apricots, apples and potatoes. 37, 429–438 (2004). https://doi.org/10.1016/j.lwt.2003.10.012
12. Khalloufi, S., El-Maslouhi, Y., Ratti, C.: Mathematical model for prediction of glass transition temperature of fruit powders. J. Food Sci. 65, 842–848 (2000). https://doi.org/10.1111/J.1365-2621.2000.TB13598.X

13. Lomauro, C.J., Bakshi, A.S., Labuza, T.P.: Evaluation of food moisture sorption isotherm equations part II: Milk, coffee, tea, nuts, oilseeds, spices and starchy foods. LWT - Food Sci. Technol. 18, 118–124 (1985)
14. Mahanti, N.K., Chakraborty, S.K., Babu, V.B.: Sorption isotherms of ready-to-puff preconditioned brown rice: Development of classical models and artificial neural network approach. J. Food Process Eng. 42, 1–11 (2019). https://doi.org/10.1111/jfpe.13220
15. Marcos, B., AsuncioZ Esteban Pascual Lo, M., AlcalaZ, M., Go, R., JoseZ Espejo, mez: Monolayer values at 30° °C of various spices as computed by the BET and GAB models. Springer-Verlag (1997)
16. McMinn, W.A.M., Al-Muhtaseb, A.H., Magee, T.R.A.: Enthalpy–entropy compensation in sorption phenomena of starch materials. Food Res. Int. 38, 505–510 (2005). https://doi.org/10.1016/J.FOODRES.2004.11.004
17. Panchariya, P.C., Popovic, D., Sharma, A.L.: Desorption isotherm modelling of black tea using artificial neural networks. Dry. Technol. 20, 351–362 (2002). https://doi.org/10.1081/DRT-120002546
18. Penner, E.A., Schmidt, S.J.: Comparison between moisture sorption isotherms obtained using the new Vapor Sorption Analyzer and those obtained using the standard saturated salt slurry method. J. Food Meas. Charact. 7, 185–193 (2013). https://doi.org/10.1007/s11694-013-9154-3
19. Rhim, J.W., Hong, S.I.: Effect of water activity and temperature on the color change of red pepper (Capsicum annuum L.) powder. Food Sci. Biotechnol. 20, 215–222 (2011). https://doi.org/10.1007/s10068-011-0029-2
20. Sahu, S.N., Tiwari, A., Sahu, J.K., Naik, S.N., Baitharu, I., Kariali, E.: Moisture sorption isotherms and thermodynamic properties of sorbed water of chironji (Buchanania lanzan Spreng.) kernels at different storage conditions. J. Food Meas. Charact. 12, 2626–2635 (2018). https://doi.org/10.1007/s11694-018-9880-7
21. Sawhney, I.K., Sarkar, B.C., Patil, G.R., Sharma, H.K.: Moisture Sorption Isotherms and Thermodynamic Properties of Whey Protein Concentrate Powder from Buffalo Skim Milk. J. Food Process. Preserv. 38, 1787–1798 (2014). https://doi.org/10.1111/jfpp.12148
22. Schmidt, S.J., Lee, J.W.: Comparison Between Water Vapor Sorption Isotherms Obtained Using The New Dynamic Dewpoint Isotherm Method and those Obtained Using The Standard Saturated Salt Slurry Method. Int. J. Food Prop. 15, 236–248 (2011). https://doi.org/10.1080/10942911003778014
23. Soysal, Y. and, Oztekin, S.: Equilibrium Moisture Content Equations for some Medicinal and Aromatic Plants. 317–324 (1999)
24. Toğrul, H., Arslan, N.: Moisture sorption isotherms and thermodynamic properties of walnut kernels. J. Stored Prod. Res. 43, 252–264 (2007). https://doi.org/10.1016/j.jspr.2006.06.006
25. Yogendrarajah, P., Samapundo, S., Devlieghere, F., De Saeger, S., De Meulenaer, B.: Moisture sorption isotherms and thermodynamic properties of whole black peppercorns (Piper nigrum L.). LWT - Food Sci. Technol. 64, 177–188 (2015). https://doi.org/10.1016/j.lwt.2015.05.045

Figures

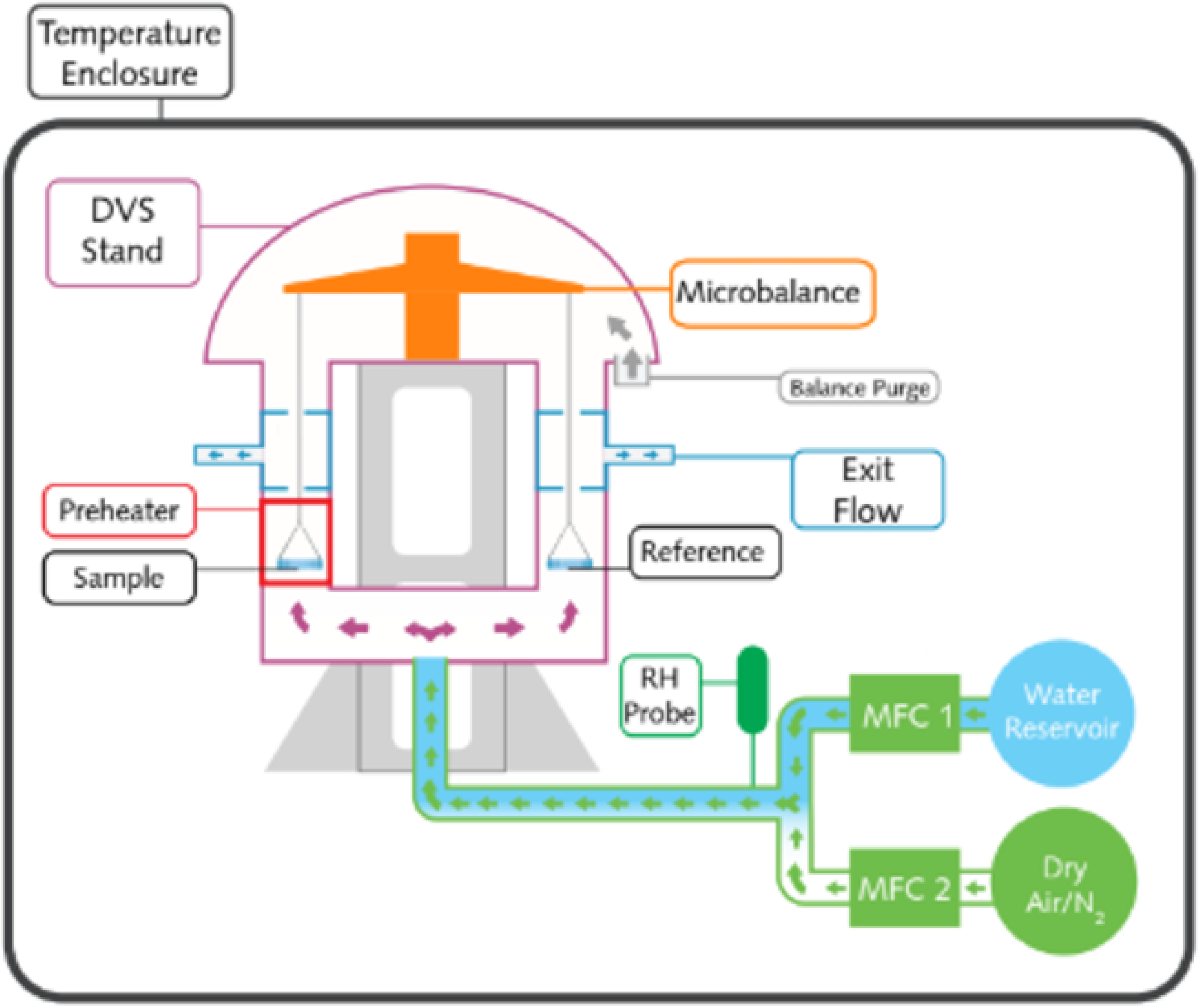

Figure 1

Schematic illustration of the basic principles of DVS instrument

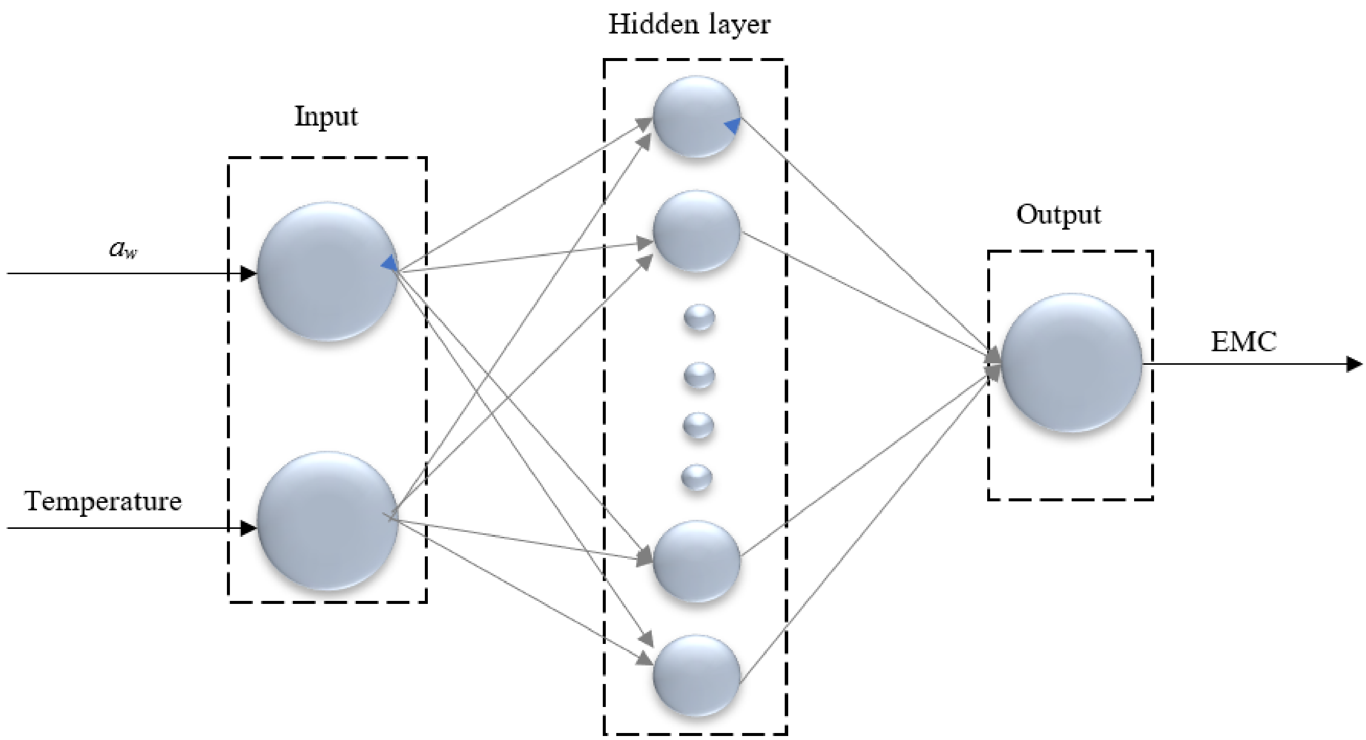

Figure 2

Schematic diagram of neural structure

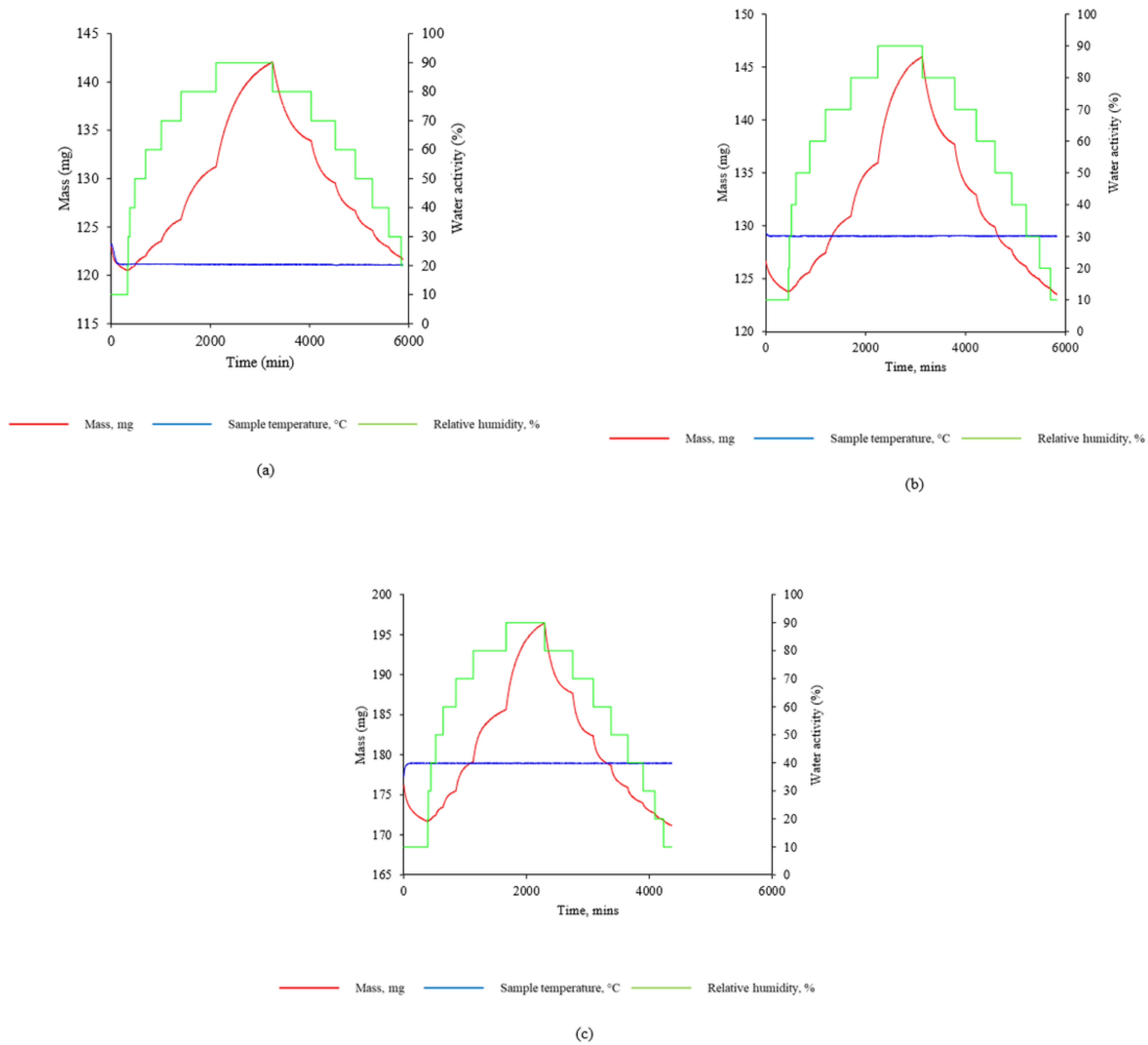

Figure 3

Temporal profile of adsorption and desorption profile of small cardamom at (a) 20, (b) 30 and (c) 40°C

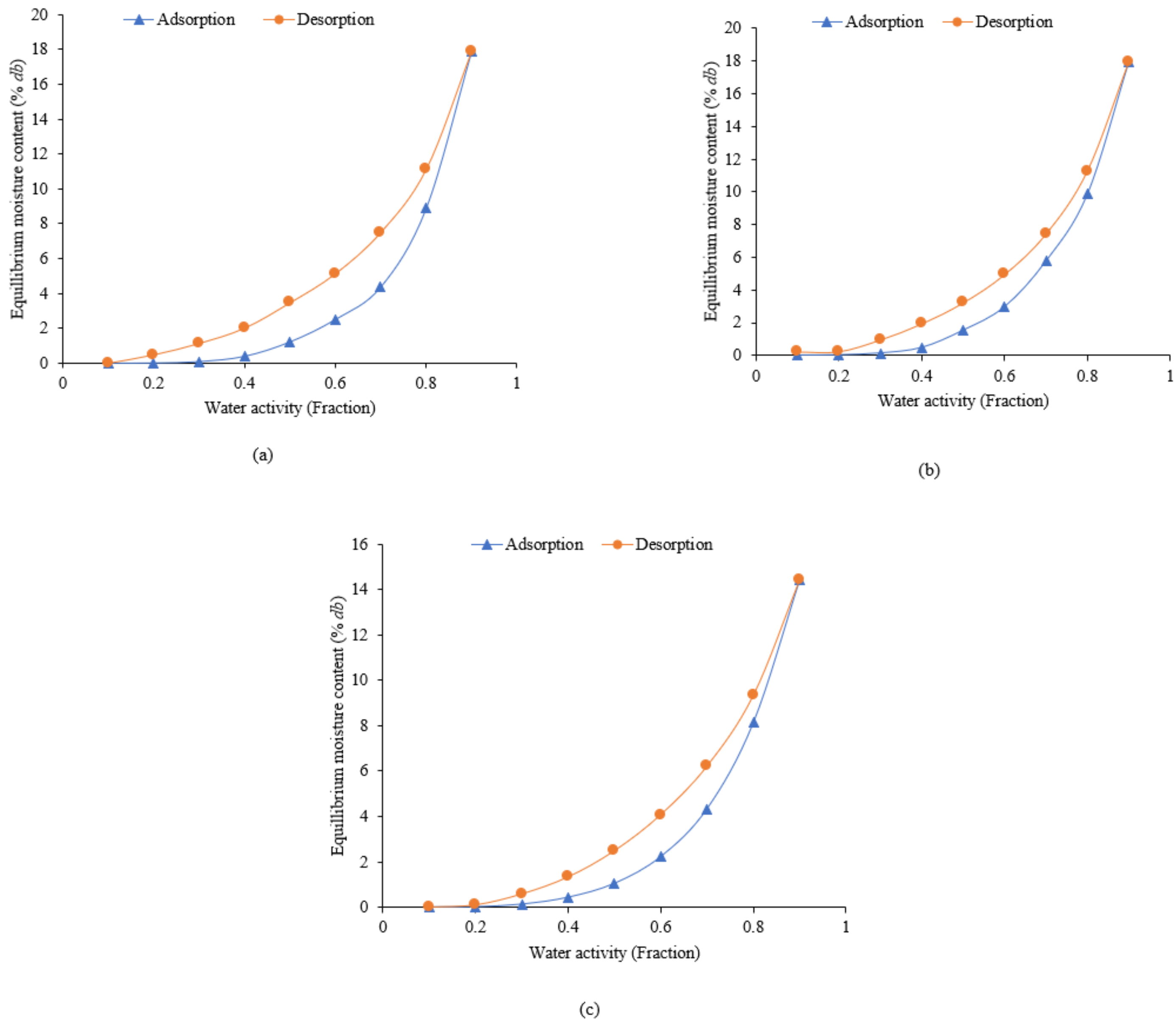

Figure 4

Moisture sorption isotherms of small cardamom at (a) 20, (b) 30 and (c) 40°C

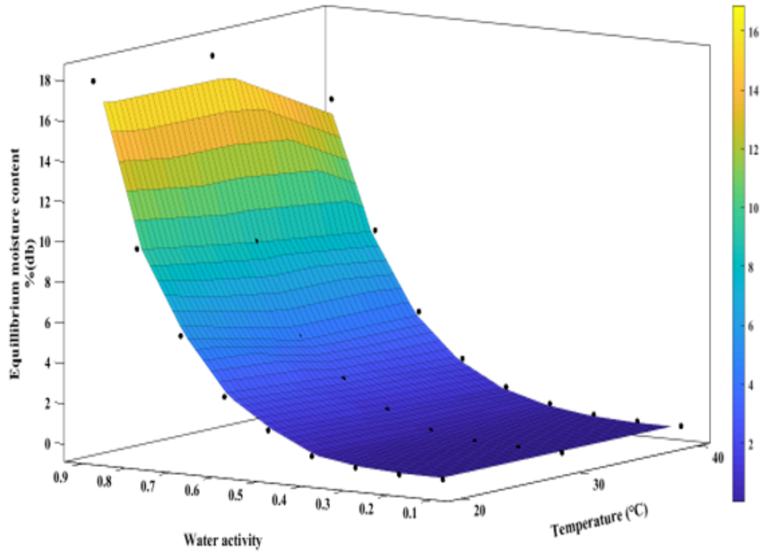

(a)

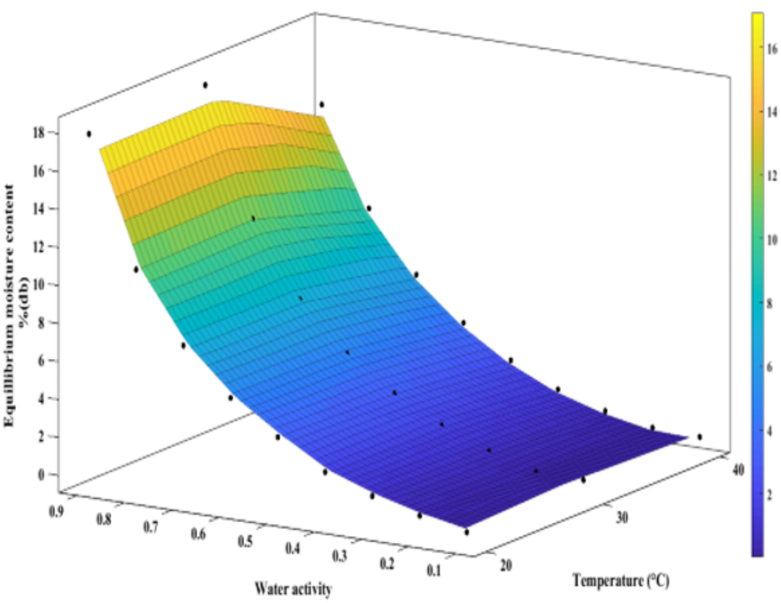

(b)

Figure 5

Effect of temperatures on (a) adsorption and (b) desorption isotherms of small cardamom

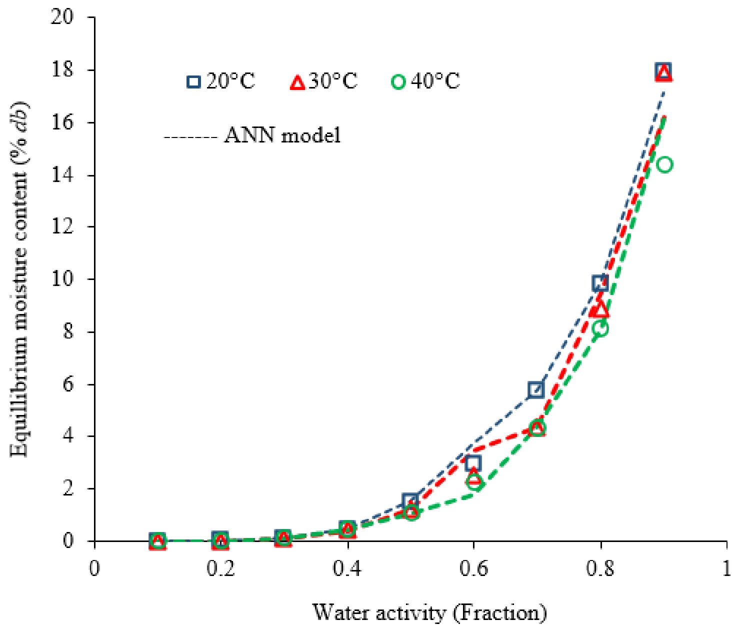

(a)

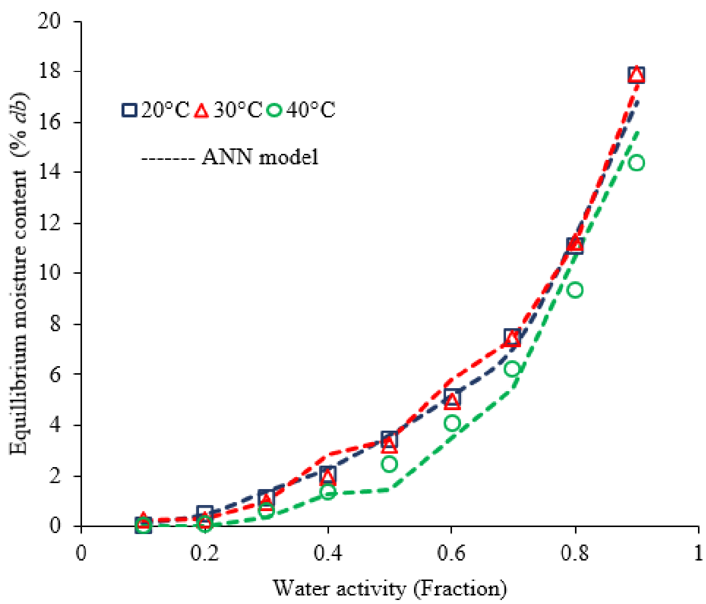

(b)

Figure 6

Experimental and predicted EMC, % (*db*) for (a)adsorption and (b)desorption proposed by ANN Model

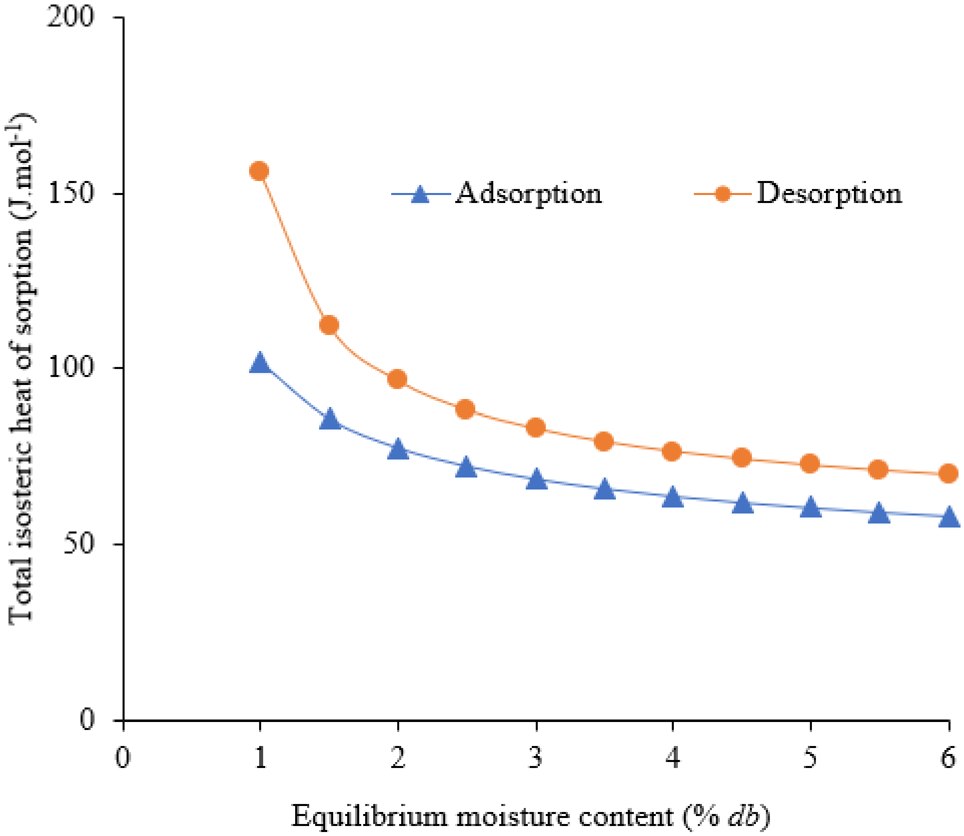

Figure 7

Effect of moisture content on the net isosteric heat of sorption of small cardamom

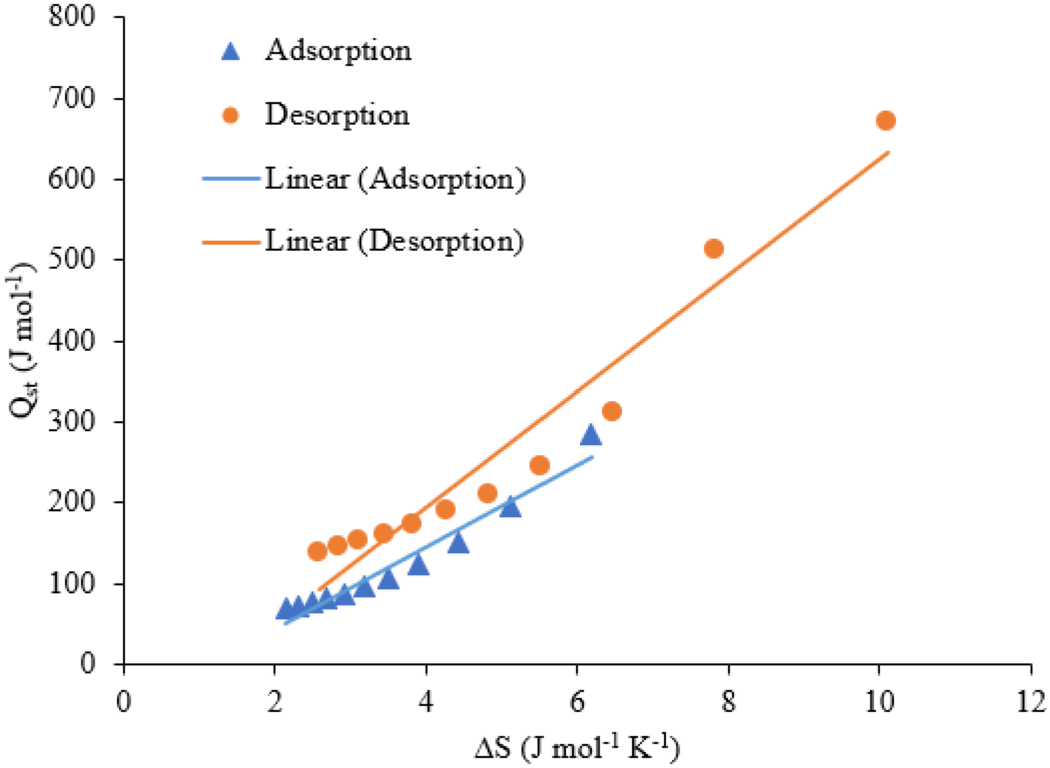

Figure 8

Enthalpy entropy compensation for small cardamom

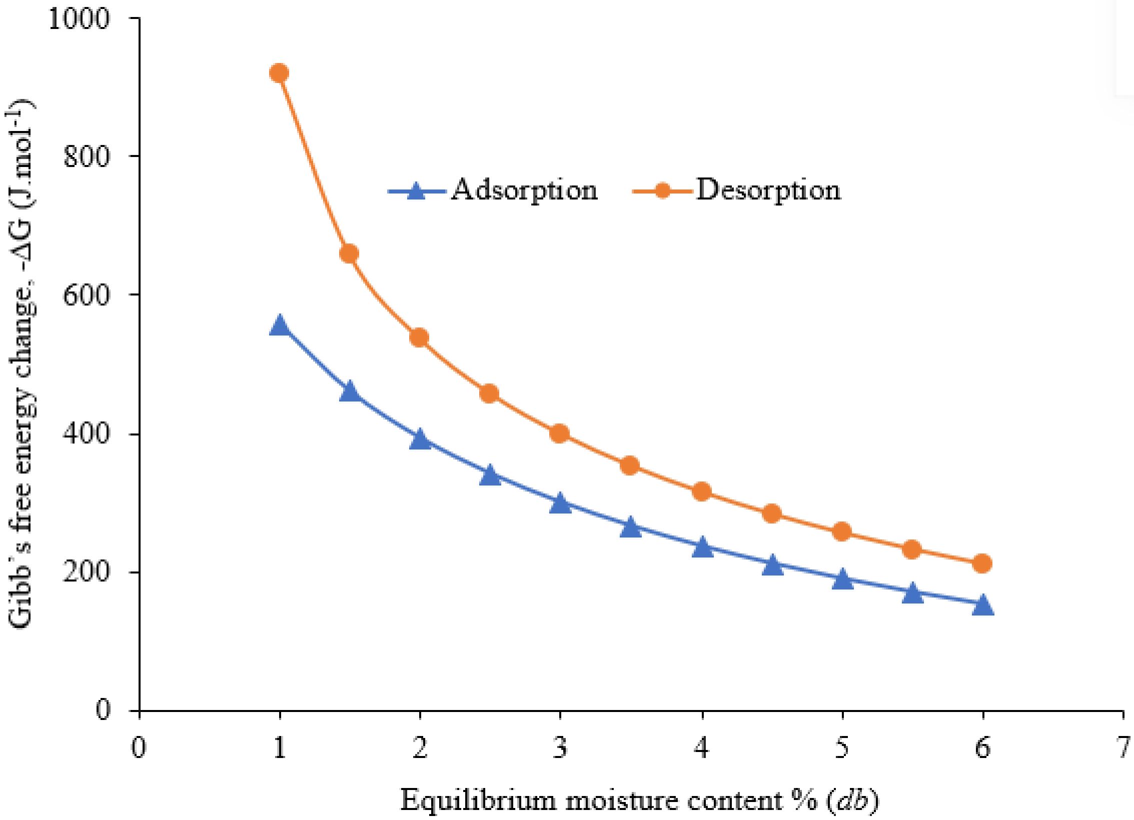

Figure 9

Variation of Gibb's free energy change with moisture content

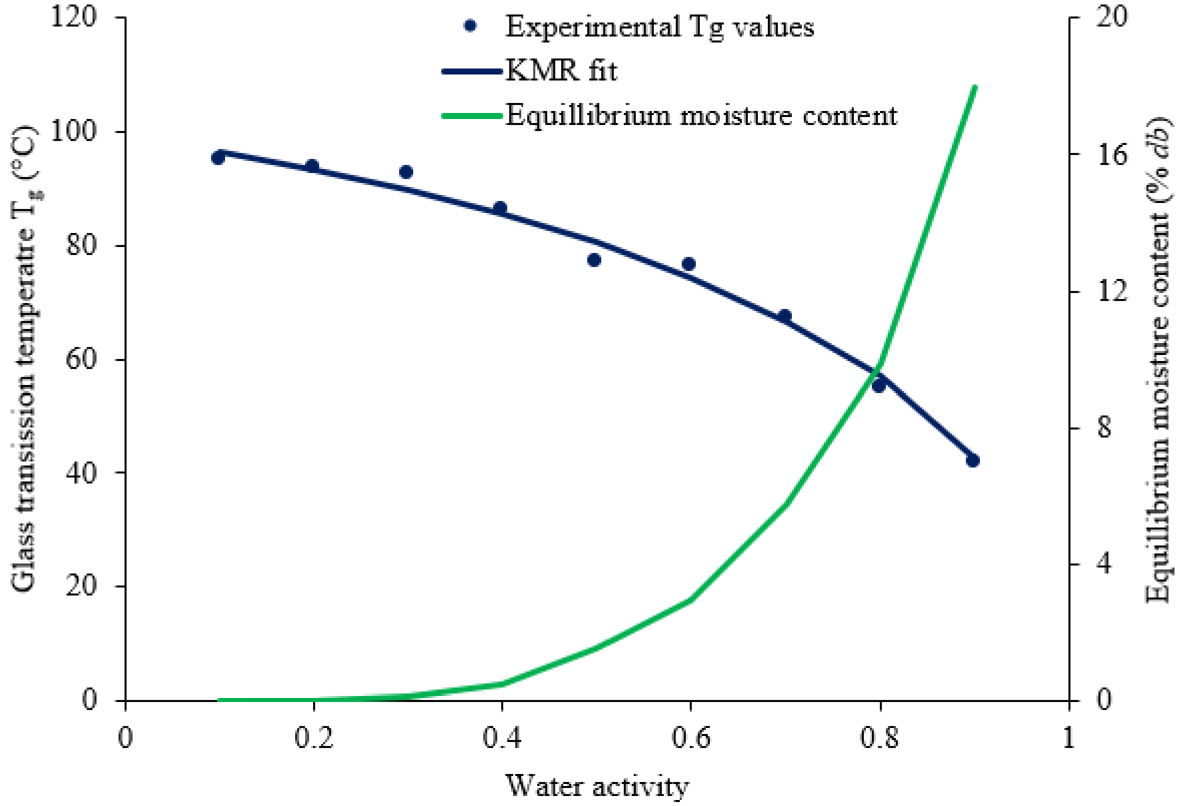

Figure 10

Glass transition and equilibrium moisture content vs. water activity